Civil Engineering Infrastructures Journal, 48(1): 101-120, June 2015
ISSN: 2322-2093

Modification of Displacement Coefficient Method in Estimation of Target Displacement for Regular Concrete Bridges Based on ASCE 41-06 Standard

Beheshti-Aval, S.B.[1*] and Jahanfekr, E.[2]

[1] Associate Professor, Civil Engineering Faculty, K.N. Toosi University of Technology, Tehran, Iran

[2] Ph.D. Candidate, Faculty of Technical and Engineering, Hormozgan University, Bandarabas, Iran

Received: 30 Sep. 2013 Revised: 30 Jan. 2015 Accepted: 4 Feb. 2015

ABSTRACT: Displacement Coefficient Method (DCM) stipulated in the ASCE 41-06 standard is becoming the preferred method for seismic rehabilitation of buildings in many high-seismic-hazard countries. Applications of the method for non-building constructions such as bridges are beyond the scope of this standard. Thus its application to this kind of structure should be approached with care. Target displacement has reasonable accuracy for buildings with strong columns and weak beams, where there is the development of plastic hinges. Due to high stiffness and strength of the deck relative to the piers in most bridges, this mechanism does not occur, and it is necessary to evaluate the accuracy of DCM for such structures. In this research, an attempt is made to evaluate the credibility of DCM in the ASCE/SEI 41-06 standard for estimating target drifts in concrete regular bridges under strong ground motions. To apply the extension of the method to bridge structures, the definition of new correction factor C_B, which should be multiplied to previous coefficients, is required. This novel coefficient can improve the accuracy of the mentioned method in accessing seismic displacement demands. The coefficient is presented for soil types A to D based on NEHRP soil classification. The validity of the modified DCM is examined for several bridges with use of nonlinear dynamic analysis. Good correlation is found between both procedures.

Keywords: Concrete Regular Bridge, Correction Factor, Displacement Coefficient Method, Nonlinear Dynamic Analysis, Nonlinear Static Analysis

INTRODUCTION

Knowledge about earthquake events is growing day by day and structural design codes are evolving accordingly. Before the 1970s, only gravity loads were utilized for design of structures. Resistance of the structure against earthquake shaking was based on design under wind lateral forces, entering into the design codes as lateral forces equal to 10% of structural weight. Since then, accepting the controlled failure of structures in severe earthquakes because of economic reasons, a new attitude has emerged. Strength reduction in relation to the elastic strength demand is commonly established through the use of the strength reduction factor (Abdollahzadeh and Malekzadeh, 2013). While strength reduction factors prescribed in seismic codes are intended to account for damping, toughness, and ductility as well as for over-strength, the level of reduction specified in seismic design codes is primarily based on observation of the performance of different structural systems

* Corresponding author E-mail: beheshti@kntu.ac.ir

in past strong earthquakes. However, this methodology also has drawbacks; in particular, structural behaviour and failure mechanisms cannot be controlled during severe earthquakes. The deficiencies pertaining to the force method led to the development of new methodology based on nonlinear analysis and considering the real behaviour of structural components during earthquake ground motions: the method of “performance-based earthquake engineering” was introduced.

Besides traffic loads, the variable and unpredictable seismic lateral forces, are the main load in the design of bridges. Most existing bridges were designed based on elastic approaches. They convey the shortcomings of this method in considering nonlinear deformation under strong ground motions, in case a lot of these structures may be vulnerable to severe earthquakes. Nonlinear dynamic analyses of existing RC bridges have proven their probable vulnerabilities against severe earthquakes. For continuing operation of infrastructure after major earthquakes, limiting damage to bridges is very important. Nonlinear seismic assessment is able to reveal the damage that may lead to failure. Using nonlinear response-history analysis is cumbersome due to several reasons, such as numerous output results, the need for powerful analysis software/professional engineers, and assessment validity under specific excitations. Application of nonlinear static analysis is simple and it is able to overcome most of the aforementioned drawbacks.

The Nonlinear Static Procedure (NSP) stipulated in current seismic rehabilitation standards has not been calibrated for bridges, and is in fact devoted to residential buildings. One of the assumptions in the development of NSP for sway structures is the occurrence of the beam sideway mechanism (total collapse) based on inducing plastic hinges at the ends of beams. This assumption is fulfilled for building structures in which the role of weak beam-strong column is acknowledged in design. But due to the long spans of bridges, their decks are much stronger than the piers under gravity loads. So, if a designer wishes to absorb seismic energy through nonlinear deformations, all these deformations should be induced in piers, which contrast the basic idea in standard NSPs. Therefore validity assessment and then accuracy augmentation, if required, are needed for application of conventional NSP for this type of structure. To this end, target displacements of nine regular bridges with different numbers of spans and pier heights on four soil types based on NEHRP soil classification were obtained and compared based on the nonlinear static procedure (NSP) versus the nonlinear dynamic procedure (NDP) stipulated in ASCE/SEI 41-06. Based on the results obtained from NDP, a correction factor was introduced. This extra coefficient should be multiplied to target displacement introduced in ASCE/SEI 41-06 to accredit this value for regular RC bridges.

PERFORMANCE-BASED EARTHQUAKE ENGINEERING OF BRIDGES

Big losses have been inflicted on countries’ economies because of failure of non-resistance bridge structures. If we consider indirect losses, such economic losses are increasing. So, assessment of seismic performance of existing bridges is an important responsibility. The major advantage of performance-based design is the condition clarification of structural performances under severe earthquakes. The performance condition is the level of damage that the structure can tolerate under considered seismic severity.

Nonlinear Static Analysis has a relatively long history; its origins may be found in research by Freeman (1975) and Fajfar (1988). But in spite of numerous studies pertaining to building structures, studies on NSP of bridges are limited.

Isakovic and Fishinger (2006) evaluated the accuracy of different pushover analysis methods, such as single-mode method, modal method, adaptive modal method, and increased-response-spectrum method, applied to bridge structures. The results showed that single-mode pushover analysis is suitable for regular bridges, and acceptable results were also found for those bridges which had moderate irregularity. However, the method had absolutely inaccurate results for irregular bridges (Lupoi et al., 2011). All methods for regular bridges had acceptable results in comparison with nonlinear response-history analysis. Zheng et al. (2003) evaluated pushover analysis application for continuous multi-span steel bridges, in which piers are reinforced by thin layers of steel. The results showed that for bridges with symmetric distribution of pier stiffness or with stiffer deck slabs relative to piers, the fundamental mode dominates the structural response and the pushover analysis can be reliably used. On the other hand, if the bridge system has asymmetric distribution of pier stiffness and relatively flexible deck slab simultaneously, higher mode effects might be significant and the accuracy of pushover analysis cannot be satisfactory. Another study, carried out by Chung and Alayed (2003), evaluated and compared parameters including target displacement, base shear and plastic-hinge rotation by the Displacement Coefficient Method (DCM). Comparing these results indicates conservative results for NSP. Shinozuka et al. (2000) implemented the Capacity Spectrum Method (CSM) to analyse girder bridges and develop their fragility curves. The results of this method were compared with the results of NTHA. Comparing fragility curves in the two methods showed desirable correlation, at least for low damage levels. For severe damage, low conformity between the two methods was observed. Fenves and Ellery (1998) used NSP for seismic evaluation of multiple-frame highway bridges in the context of the 1994 Northridge earthquake. Pushover analysis gave a good estimation for the capacity of piers and enabled the definition of performance level for each component and the determination of the most likely cause of failure. The pushover analysis showed failure occurred in the pier before reaching target displacement. In the study by Paraskeva et al. (2006), the development of pushover analysis method regarding higher modes is considered. The results for lateral displacement of end-bridge nodes had the most differences between NSP and NTHA. The obtained displacement of modal pushover analysis (MPA) had better correlation with the results of NRHA. The adaptive pushover applied to bridges by Pinho et al. (2007) showed good results for common bridges and presented fair results with reasonable accuracy for irregular bridges.

Nonlinear Static (Pushover) Method

Pushover analysis is a static, nonlinear procedure in which the magnitude of the lateral seismic loading is incrementally increased in accordance with a certain predefined pattern until predetermined displacement reaches a target value or failure modes occur. It promises to be a useful and effective tool for performance-based design.

The principle of this method shows one mathematic model with nonlinear behaviour of structure affected by lateral load pattern and increasing with constant mode until the certain node of the structure (the centre of mass of the bridge deck) reaches the target displacement. During the process of increasing lateral load, the strength and stiffness of structural components in every step are corrected according to their inherent nonlinear behaviour. The main product of this process is the curve of base shear versus controlling point displacement, which is defined as structure capacity curve, in which every point indicates special structural damage. In this study the total base shear is the summation of the base shears in piers and abutments in the transverse direction of the bridge, which is calculated based upon Eq. (1). The displacement refers to the displacement component in the transverse direction. The position of target displacement is determined at the centre of mass of the bridge deck (Figure 1).

$$V = \sum_{i=1}^{n} H_i = \sum_{j=1}^{m} R_j \qquad (1)$$

where i: is number of nodes, j: is number of supports, R_j: is reaction force at support j, H_i: is force at node i and V: is total base shear.

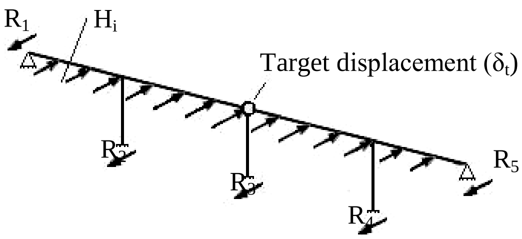

Fig. 1. Summations of support reactions as the base shear and target displacement at center of mass.

EVALUATION OF TARGET DISPLACEMENT BASED ON DCM IN FEMA 356 DOCUMENT AND ASCE 41-06 STANDARD

The purpose of using seismic rehabilitation standards is to apply concerted references for seismic evaluation of existing buildings. In NSP as presented in the FEMA 356 document, a displacement coefficient method is utilized. The target displacement is evaluated based on modification of elastic equivalent SDOF with coefficients C_0-C_3 according to Eq. (2). The target displacement shows the average maximum displacement of structure during probable earthquakes. A detailed description can be found in FEMA 365. This standard was improved in FEMA 440 and incorporated in ASCE/SEI 41-06 standard.

$$\delta_t = C_o\, C_1\, C_2\, C_3\, S_a \frac{T_e^{\,2}}{4\pi^2} g \qquad (2)$$

where C_0: is modification factor to relate spectral displacement of an equivalent SDOF system to the roof displacement of the building MDOF system, C_1: is modification factor to relate expected maximum inelastic displacements to displacements calculated for linear elastic response, C_2: is modification factor to represent the effect of pinched hysteretic shape, stiffness degradation and strength deterioration on maximum displacement response, C_3: is modification factor to represent increased displacements due to dynamic P-Δ effects, S_a: is response spectrum acceleration at the effective fundamental period and damping ratio of the building in the direction under consideration, T_e: is effective fundamental period of the building in the direction under consideration and g: is acceleration of gravity.

Coefficient C_3 was eliminated in ASCE/SEI 41-06 and replaced with a limit on minimum strength (maximum R) required, avoiding dynamic instability.

Lateral Load Patterns

The lateral load patterns applied in structures indicate predominating distribution of inertia forces during earthquakes. The distribution of these forces will vary continuously during earthquake response as portions of the structure yield and stiffness characteristics change. The extremes of this distribution will depend on the severity of the earthquake shaking and the degree of nonlinear response of the structure (Shayanfar and Rezaei Abyaneh, 2011). The first step in NSP is pushing the structure by lateral forces with an invariant height-wise distribution until a predetermined target displacement is reached.

It is obvious that different lateral load patterns yield different capacity curves. General non-acknowledgement of lateral load pattern is a weakness of NSP (in fact the nature of seismic load is variable). A previous study on regular concrete bridges (Jahanfekr, 2011) and a provision included in ASCE/SEI 41-06 recommend utilizing a vertical distribution proportional to the shape of the fundamental mode. Therefore, in this paper, load pattern based on first mode has been used for developing capacity curve. There are two patterns for lateral load distributions on the bridge. The first applies loads only on the deck slab, and the second on the deck and the piers simultaneously. In this research, because of mass concentration in the deck, the first method has been used with acceptable approximation (Figure 2).

MODELLING HYPOTHESIS

The studied bridges in this research are concrete regular bridges, with equal spans of 15 m, two, three, four, five and six in number, respectively. The heights of bridge piers are 5, 8, 12, 20 and 30 m. The piers are reinforced by 36-mm-diameter rebar and have a longitudinal reinforcement ratio of 1–2.5%. All bridges are loaded and designed according to the AASHTO (2010) Standard Specifications. The superstructure is a cast-in-place concrete slab integrated with longitudinal girders with T-shaped cross-sections. The number of longitudinal girders for all models is six and the distance between longitudinal girders is 1.8 m; the predicted distance between sidewalks is 9.4 m. The assumed asphalt layer thickness is 7 cm. The total width of bridges is 11 m and two traffic lanes are considered for all the models. Three equal-spaced circular piers in each rectangular cap beam transfer gravity loads to ground. The seat-type abutments allow free longitudinal movement of the superstructure and do not provide longitudinal restraint. In the transverse direction, the superstructure is assumed to act simply as a supported beam spanning laterally between the abutments with the maximum transverse displacement at the centre of the middle span. A shear key provides transverse restraint to enable transfer of transverse seismic forces to the abutment.

The T-girder and slab deck are continuous over cap beams; thus full continuity is employed at the superstructure-bent intersection. All bridges are modelled in three dimensions by the software OpenSees^{TM}. This software is appropriate for nonlinear static and dynamic analysis of RC concrete structures.

The translation and rotation fixed ends are considered for attachment of piers to the foundations (Figure 3). The support stiffness specifications for piers and abutments are shown in Table 1. The isometric and elevation view of the bridges, deck cross-section, bridge cross-section in relation to frames location, and typical cross-section shapes of piers are displayed in Figures 4 to 8, respectively. Specifications of deck, cap-beam and piers cross-sections are depicted in Tables 2 and 3. x, y and z axes are defined as follows:

x axis: set in longitudinal direction of bridge;

y axis: set in transverse direction of bridge;

z axis: set in vertical direction of bridge.

(a) Lateral loads on the deck slab **(b)** Lateral loads on the deck slab and the piers

Fig. 2. Two alternatives for lateral load distributions (Jahanfekr, 2011).

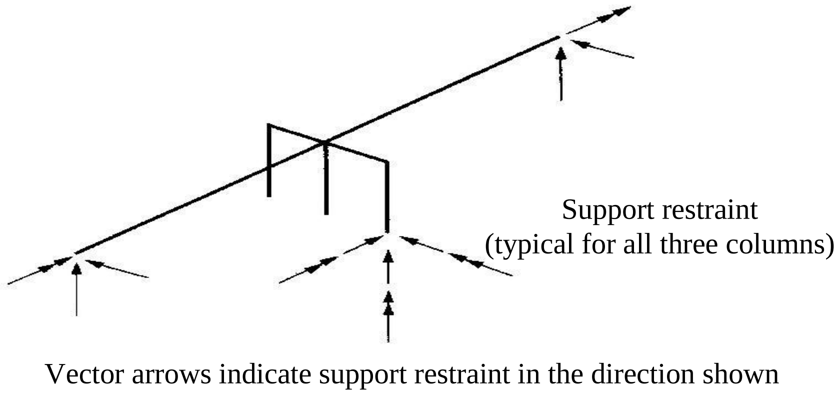

Fig. 3. Support conditions for piers and abutments model.

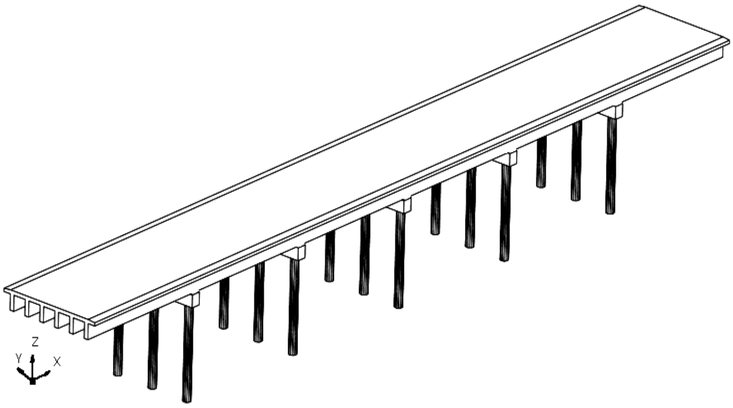

Fig. 4. Isometric view of a sample bridge.

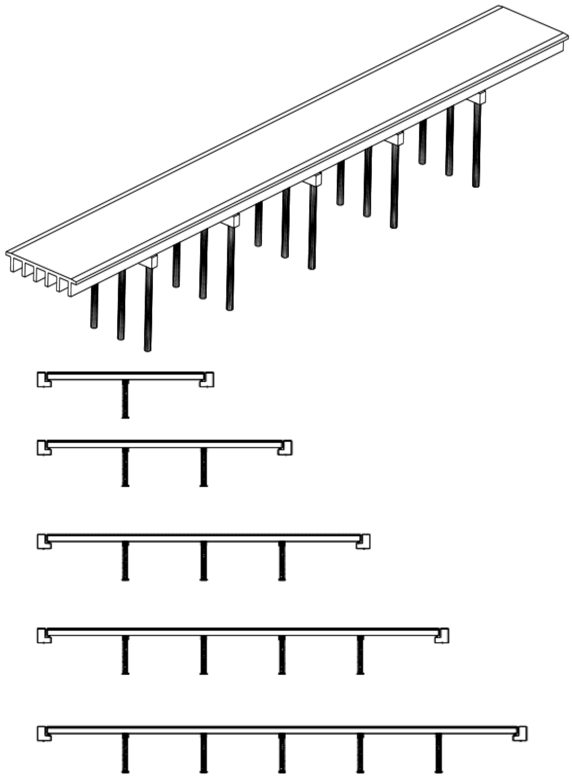

Fig. 5. Elevation of bridges in longitudinal direction.

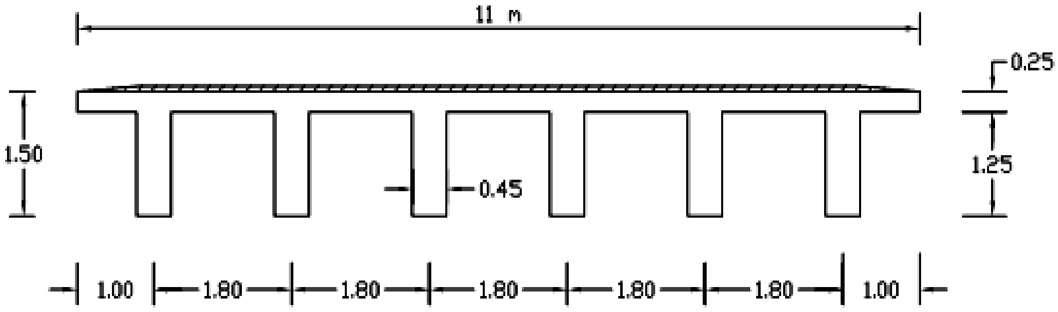

Fig. 6. Deck cross section.

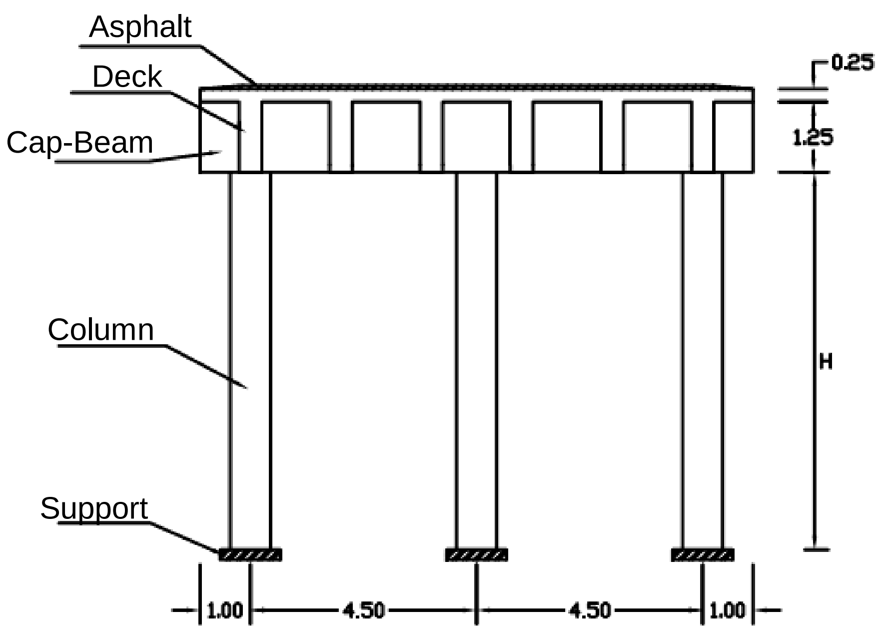

Fig. 7. Bridge cross section.

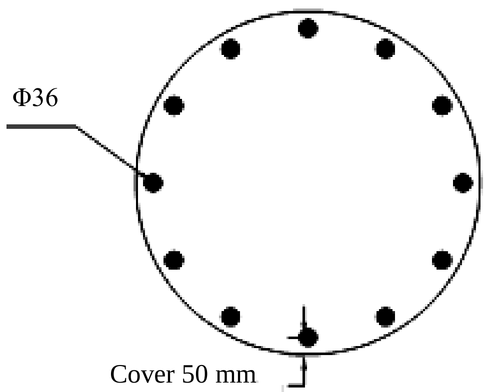

Fig. 8. Typical cross-section shapes of bridge pier.

Table 1. The support stiffness for the analytical models.

	k_x	k_y	k_z	k_{rx}	k_{ry}	k_{rz}
Piers	∞	∞	∞	∞	∞	∞
Abutments	0	∞	∞	∞	0	0

Table 2. The specifications of bridge pier cross sections (Jahanfekr, 2011).

No. of Spans	High Pier (m)	N. ω 36	ρ	D_{col} (m)	A (cm^2)	I_{2-2}, I_{3-3} (cm^4)	J (cm^4)
2	8	12	1.92	0.9	6362	3220631	6441262
3	8	12	1.56	1	7854	4908750	9817500
4	8	14	1.81	1	7854	4908750	9817500
5	8	12	1.92	0.9	6362	3220631	6441262
6	8	10	1.60	0.9	6362	3220631	6441262
6	5	10	2.03	0.8	5027	2010624	4021248
6	12	12	1.56	1.3	13273	14019881	28039762
6	20	18	1.38	1.4	15394	18857454	37714908
6	30	34	1.36	1.8	25447	51530094	103060188

Table 3. The specifications of the deck and the cap-beam cross sections (Jahanfekr, 2011).

Deck cross-section	**A (m^2)**	**I_{2-2} (m^4)**	**I_{3-3} (m^4)**	**J (m^4)**
	6.125	59.68	1.31	0.31
Cap-Beam cross-section	**L (m)**	**B (m)**	**H (m)**	**A (m^2)**
	10	D_{col} + 0.5	1.25	variant

Due to high stiffness and yield strength of deck and cap-beams in comparison to piers, these elements are modelled with a linear-elastic beam element. Determination of the moment of inertia and torsional stiffness of the superstructure is based on un-cracked cross-sectional properties, because the superstructure is expected to respond linearly to seismic loadings (Aviram et al., 2008; Elgamal et al., 2008; Yan, 2006). The analysed stresses in the bridge deck with beam showed the credibility of this assumption.

As shown in Figure 9, the model includes the space frame, which is regarded as a two-node line element in the Finite Element Analysis. Each of the nodes has six degrees of freedom. The superstructure is modelled with six elements per span located along the centroid of the superstructure. The total mass of the structure is lumped to the nodes of the superstructure and weight of the cap beams and half-weight of the piers lumped to nodes of the superstructure corresponding to piers.

In this research, the confined concrete stress-strain is determined from the confined concrete model developed by Mander et al. (1998). The constitutive model used for the steel reinforcement is a simple elastic-plastic bilinear model. The steel has initial stiffness E=2.0 MPa and post-yield hardening stiffness of 2% pre-yield stiffness. Sample confined and unconfined concrete and steel stress-strain relationships are shown in Figures 10, 11 and 12, respectively. The piers are modelled using fully three-dimensional nonlinear beam-column fibre elements (Figure 13). Nonlinear geometry effects are applied through inclusion of P-Δ effects in addition to material nonlinearity to the bridge models.

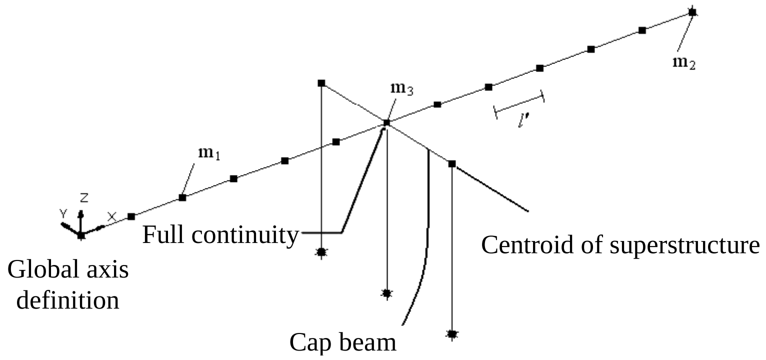

Fig. 9. The method of positioning and distribution of masses in different nodes of bridge.

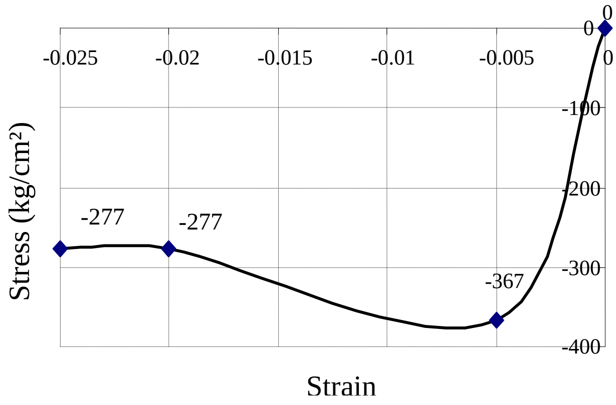

Fig. 10. Confined concrete constitutive relationships (core).

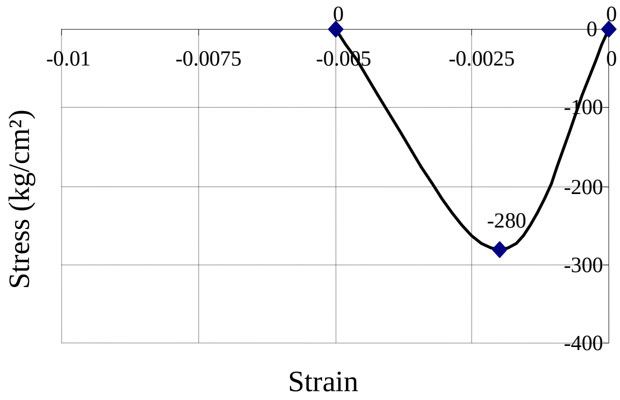

Fig. 11. Unconfined concrete constitutive relationships (cover).

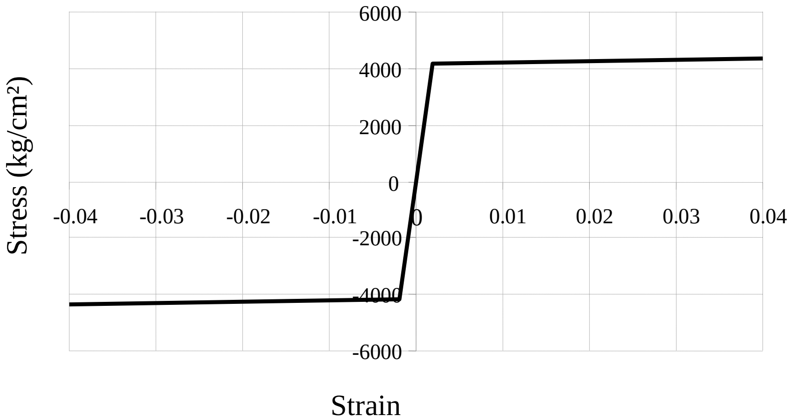

Fig. 12. Reinforcing steel constitutive relationships.

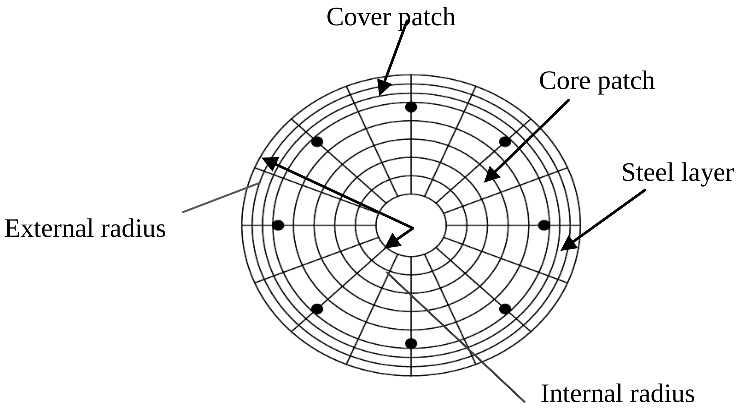

Fig. 13. Typical discretization of a typical pier cross-section into fiber.

Stiff elements (with increased stiffness properties) are used to model the cap beams for distribution of loads between the columns without deformation in the cap beams in order to match the behaviour of the superstructure.

In the analytical model, mass and stiffness proportional damping (Rayleigh damping assumption) is used to determine the damping of all elements. In this method, mass and stiffness proportional coefficients are specified according to the calculated periods of the first and third transverse modes. Furthermore, 5% Rayleigh damping ratio is assumed in the analysis for each mode.

EVALUATION OF CURRENT DCM APPLIED TO BRIDGES

In the first step of this study, target displacement obtained from DCM of FEMA 356 and ASCE/ SEI 41-06 is compared with the corresponding value resulting from NDP, which is considered the most accurate and reliable procedure. Comparison of results is carried out in order to assess the accuracy of DCM in estimating target displacement of bridges. To take care of the uncertainty associated with each time-history record, the average of maximum displacements resulting from the seven time-histories for each soil type according to NEHRP soil classification (A-B-C-D) is implemented for the comparison with the NSP results (Tables 4-7). The records are selected with magnitude 6–7.6 Richter and distance 50–100 km from fault. These records are extracted from the PEERS website. Each of the four groups is normalized with the unit-energy method based on Eq. (3) (Lestuzzi et al., 2004). The base-design spectral acceleration (A) for high-seismic-risk regions of Iran is considered as 0.35 (Iranian seismic code, 2800). The acceleration-response spectrums of normalized records and their averages are shown for the four groups in Figure 14. In order to involve inherent characteristics of ground-motion excitations in the presentation of maximum displacement ratios, periods of vibration were normalized by the predominant period of the ground motion, as first proposed by Miranda (1993). The predominant period, T_g of the ground motion is computed as the period of maximum relative velocity of a 5% damped linear-elastic system throughout the whole period range. Examples of the computation of T_g for one record belonging to the far-field ground motion set are shown in Figure 15.

$$PGA_{Correct} = \left[\frac{Area_{spectrum}}{Area_{record}}\right] A \qquad (3)$$

where $PGA_{Correct}$: is normalized peak acceleration, $Area_{Spectrum}$: is area under design acceleration spectrum for (ξ=5%), normalized to unit peak acceleration, $Area_{Record}$: is area under record acceleration spectrum for (ξ=5%), normalized to unit peak acceleration (before normalizing), and A: is design base acceleration.

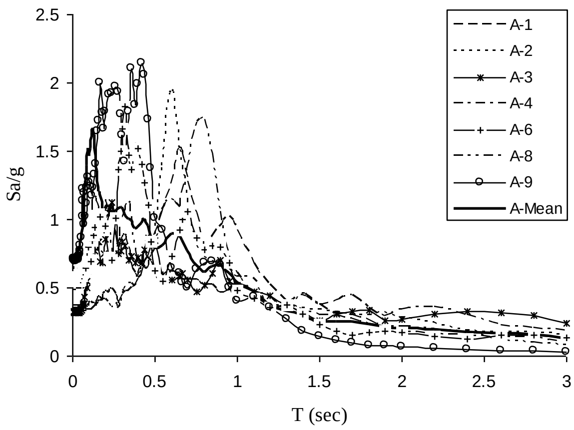

Soil type (A) or (I)

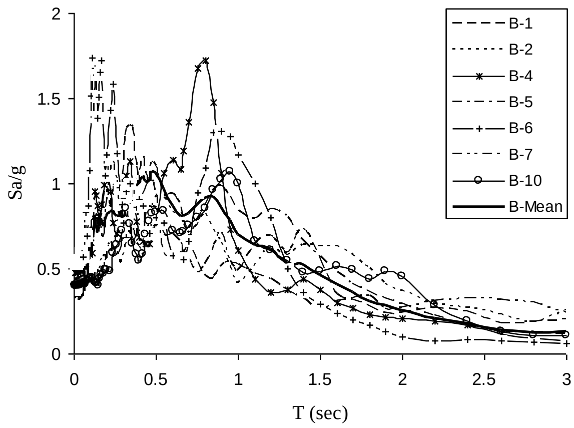

Soil type (B) or (II)

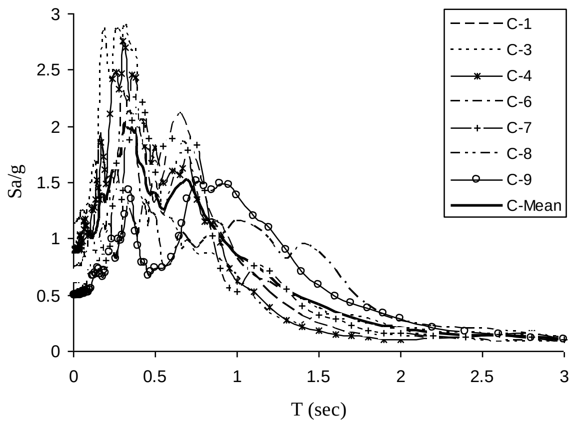

Soil type (C) or (III)

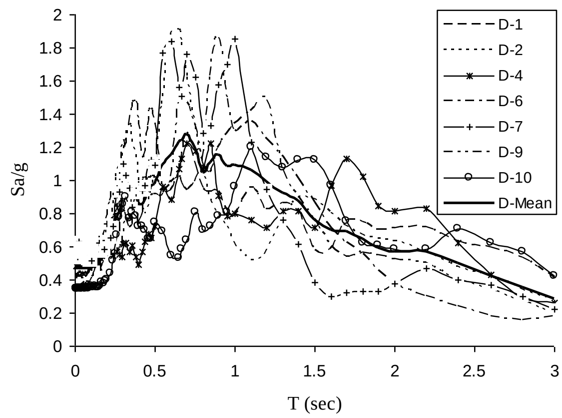

Soil type (D) or (IV)

Fig. 14. Normalized acceleration response spectrums for different soils (ξ=5%).

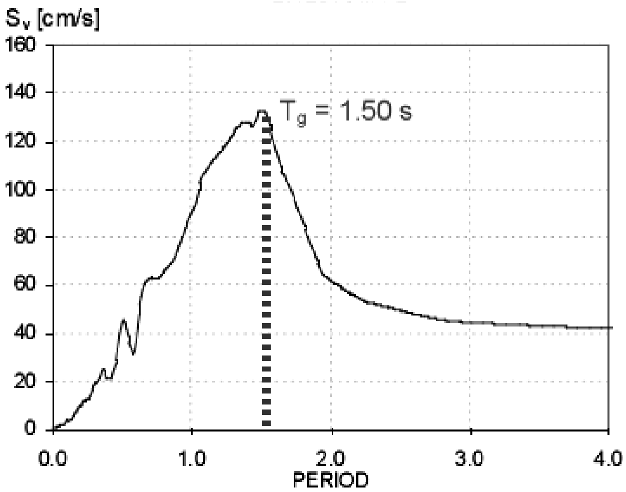

Fig. 15. Predominant ground motion period for the assumed soil record obtained from PEER website.

Table 4. Set of ground motion records in soil type A.

ID Record	Record, Component	M (Richter)	D (Km)	PGA (g)	PGV (cm/s)	PGD (cm)
A-1	CHICHI, TAP103-N	7.6	125.5	0.177	21.7	8.93
A-2	CHICHI, TAP103-W	7.6	125.5	0.122	22.7	8.32
A-3	LANDERS, ABY000	7.3	69.2	0.115	18.3	11.16
A-4	LANDERS, ABY090	7.3	69.2	0.146	20	7.38
A-6	LOMAP, SSF205	6.9	68.2	0.105	8.8	4.59
A-8	PALMSPR, H02090	6	57.6	0.093	1.8	0.29
A-9	NORTHR, BAL090	6.7	71.5	0.08	3.8	0.56

Table 5. Set of ground motion records in soil type B.

ID Record	Record, Component	M (Richter)	D (Km)	PGA (g)	PGV (cm/s)	PGD (cm)
B-1	CHICHI, CHY074-N	7.6	82.5	0.158	23.6	11.74
B-2	CHICHI, CHY074-W	7.6	82.5	0.234	28.1	19.04
B-4	LANDERS, BOR000	7.3	90.6	0.119	12.9	9.14
B-5	LOMAP, GGB270	6.9	85.1	0.233	38.1	11.45
B-6	LOMAP, HWB220	6.9	58.9	0.159	15.1	3.72
B-7	PALMSPR, ATL270	6	55.4	0.11	6.5	0.71
B-10	NORTHR, NEW090	6.7	84.6	0.103	5.8	1.21

Table 6. Set of ground motion records in soil type C.

ID Record	Record, Component	M (Richter)	D (Km)	PGA (g)	PGV (cm/s)	PGD (cm)
C-1	WHITTIER, A-BIR090	6	56.8	0.243	13.7	1.92
C-3	NORTHR, BRC090	6.7	61.6	0.206	12.3	1.23
C-4	NORTHR, SSE330	6.7	60	0.194	12.1	2.28
C-6	LOMAP, TIB270	6.9	77.4	0.244	36.1	7.2
C-7	COALINGA, H-C08270	6.4	50.7	0.1	8	1.25
C-8	IMPVALL, H-VCT345	6.5	54.1	0.167	8.3	1.05
C-9	CHICHI, HWA045-N	7.6	73.34	0.183	26.9	19.31

Table 7. Set of ground motion records in soil type D.

ID Record	Record, Component	M (Richter)	D (Km)	PGA (g)	PGV (cm/s)	PGD (cm)
D-1	MORGAN, A01310	6.2	54.1	0.068	3.9	0.63
D-2	LOMAP, TRI090	6.9	82.9	0.159	32.8	11.52
D-4	DUZCE, ATS030	7.1	193.3	0.038	7.4	5.07
D-6	KOCAELI, ATS090	7.4	78.9	0.184	33.2	25.83
D-7	CHICHI, TAP095-E	7.6	111.56	0.151	26.9	13.37
D-9	CHICHI, TAP090-E	7.6	111.98	0.131	31.9	13.73
D-10	CHICHI, TAP003-E	7.6	104.34	0.126	34.8	20.61

In the second step, the new corrective coefficient C_B, multiplied by the previous coefficients, is introduced for the concrete regular bridges to see whether the modified formula for estimation of target displacement could increase the accuracy of DCM as stipulated in ASCE/SEI 41-06. Again, the overall results are valid for concrete regular bridges with short and medium length in regions far from active faults.

RESULTS EVALUATION

The accuracy of standard DCM in estimation of target displacement changes with records and structural specifications. In order to make a fair judgement about the accuracy of DCM, the points corresponding to pair values $(T_e/T_g\ ,(Dis_i)_{NDP}/(Dis_i)_{NSP})$ are drawn in Figure 16. As can be seen, the horizontal axis is the ratio of effective period in transverse direction of bridges to earthquake-record predominant periods T_e/T_g , and the vertical axis is the ratio of maximum displacement of NDP in transverse direction to NSP target displacement $(Dis_i)_{NDP}/(Dis_i)_{NSP}$ based on Eq. (2) for the two aforementioned standards. Obviously each set of values $(Dis_i)_{NDP}/(Dis_i)_{NSP}$ close to one for different T_e/T_g has better prediction accuracy. Values under one indicate overestimation and above one underestimation in comparison with accurate NDP. The accuracy of the FEMA 356 pre-standard and the ASCE/SEI 41-06 standard in predicting target displacement is shown for different soils in Table 8.

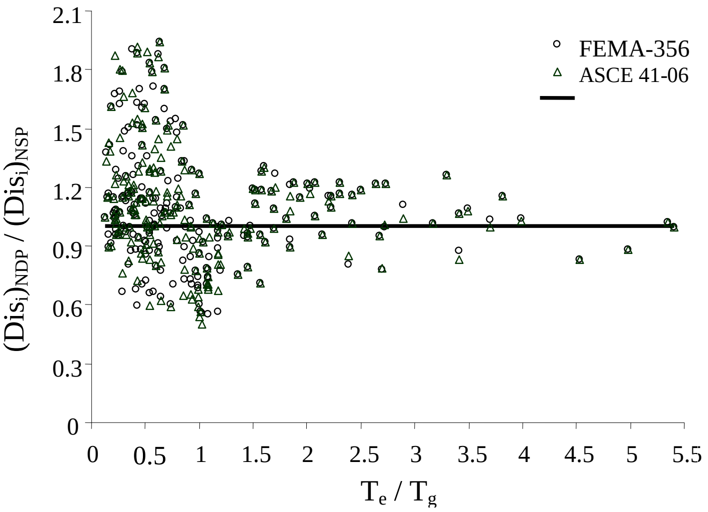

Fig. 16. The general comparison between the values of $(Dis_i)_{NDP}/(Dis_i)_{NSP}$ for every four soils in selected bridges for FEMA 356 document and ASCE 41-06 standard.

Table 8. The average values and standard deviations for soil types.

Soil Type	Method	$\bar{X}$	σ	$(\bar{X}-1)\%$
A	FEMA 356	1.080	0.305	8
	ASCE 41-06	1.064	0.307	6.41
B	FEMA 356	1.234	0.429	23.4
	ASCE 41-06	1.218	0.410	21.8
C	FEMA 356	1.091	0.355	9.1
	ASCE 41-06	1.087	0.345	8.7
D	FEMA 356	1.382	0.632	38.2
	ASCE 41-06	1.191	0.452	19.1

In this table $\bar{X}$ and σ are the average and standard deviation of the results of NSP in comparison with the results of NDP.

Comparison of the results between the FEMA 365 document and the ASCE/SEI 41-06 standard indicates closeness for soil type D. It seems the correction of coefficients in ASCE/SEI 41-06 could not increase the accuracy of the estimated target displacement for the bridges in this research. Furthermore, both FEMA 365 and ASCE/SEI 41-06 incorporate more errors for bridges in soil types B and D. Table 8 shows that ASCE/SEI 41-06 could improve the results' accuracy for soil type D.

Accuracy estimation of target displacement by both FEMA 356 and upgrade version i.e., ASCE/SEI 41-06, indicated that incorporated DCM was unqualified to assess seismic displacement demand for certain bridge structures studied in this research. This inconsistency may be due to differences in failure and energy-dissipation mechanisms and also different transfers of earthquake shear into ground in comparison with buildings. Unfortunately the MDOF-frame dissipating mechanism for estimation of target drift (Eq. (2)) has not been incorporated in these documents. The C_1 and C_2 coefficients are obtained based on SDOF systems in which the mechanism type of MDOF structure in nonlinear deformation range cannot be included in these coefficients. Application of DCM for bridges is beyond the scope of this standard. The standard basically allows us to expect reasonable accuracy in target displacement for frames with weak beams and strong columns, with induced plastic hinges at the beam ends under strong seismic lateral loads. Due to high stiffness and strength of the deck system relative to the piers in common bridges, the mentioned mechanism does not occur. It is necessary to add an extra coefficient to consider induced plastic hinges at the bridge pier ends (dependent on axial force level) instead of the deck ends.

In this research, the additional correction factor C_B is introduced for regular RC bridges to augment the accuracy of current DCM in ASCE/SEI 41-06. This coefficient may be considered as the influence of the type of dissipating mechanism on target displacement.

Referring to Figure 16, the ratio $(Dis_i)_{NDP}/(Dis_i)_{NSP}$ is identical to correction factor C_B, which we are looking for. However, when the span number was altered, the ductility of the bridge structures slightly changed. So, the correction factor was solely introduced as a function of T_e/T_g, dependent on structural effective period and ground motion characteristics. Twenty-eight seismic records selected from four soil types were applied to 25 designed bridges. Seven hundred dynamic analyses for calculation of maximum displacement were accomplished and corresponding target displacements were estimated from Eq. (2). The curve-fitting process was used to find the best correlation to obtain C_B versus T_e/T_g. These curves and their mathematical description are shown in Figure 17 and Eqs. (4–7) for the four soil types respectively.

$$C_B = \begin{cases} 0.0375\left(\frac{T_e}{T_g}\right)^2 - 0.3609\left(\frac{T_e}{T_g}\right) + 1.1548 & \frac{T_e}{T_g} \le 1.3 \\ -0.0811\left(\frac{T_e}{T_g}\right)^2 + 0.4821\left(\frac{T_e}{T_g}\right) + 0.4225 & 1.3 \le \frac{T_e}{T_g} \le 4 \end{cases} \tag{4}$$

$$C_B = \begin{cases} 3.1397\left(\frac{T_e}{T_g}\right)^2 - 0.8443\left(\frac{T_e}{T_g}\right) + 1.0835 & \frac{T_e}{T_g} \le 0.8 \\ -0.3509\left(\frac{T_e}{T_g}\right)^2 + 1.4433\left(\frac{T_e}{T_g}\right) - 0.2634 & 0.8 \le \frac{T_e}{T_g} \le 2.5 \end{cases} \tag{5}$$

$$C_B = \begin{cases} 1.7073\left(\frac{T_e}{T_g}\right)^2 - 3.208\left(\frac{T_e}{T_g}\right) + 2.2964 & \frac{T_e}{T_g} \le 0.8 \\ -0.1027\left(\frac{T_e}{T_g}\right)^2 + 0.6728\left(\frac{T_e}{T_g}\right) + 0.2362 & 0.8 \le \frac{T_e}{T_g} \le 2.2 \end{cases} \tag{6}$$

$$C_B = \begin{cases} -1.0983\left(\frac{T_e}{T_g}\right)^2 - 4.8815\left(\frac{T_e}{T_g}\right) + 3.2666 & \frac{T_e}{T_g} \le 0.5 \\ -0.7341\left(\frac{T_e}{T_g}\right)^2 + 2.8685\left(\frac{T_e}{T_g}\right) - 0.33 & 0.5 \le \frac{T_e}{T_g} \le 1 \\ -0.8952\left(\frac{T_e}{T_g}\right)^2 + 3.0891\left(\frac{T_e}{T_g}\right) - 1.5844 & 1 \le \frac{T_e}{T_g} \le 1.8 \end{cases} \tag{7}$$

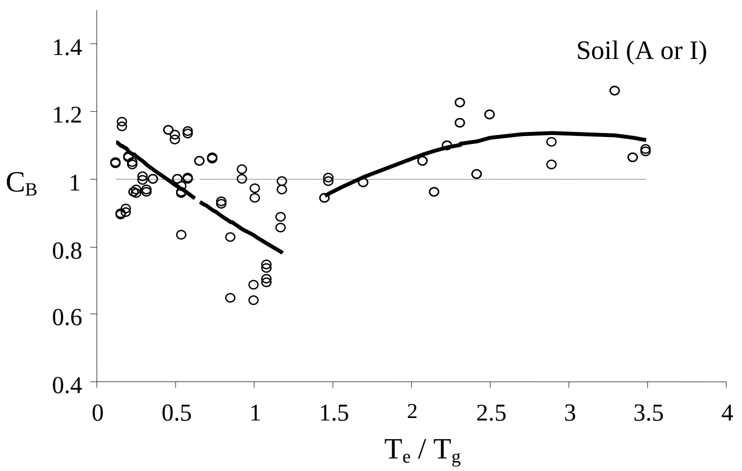

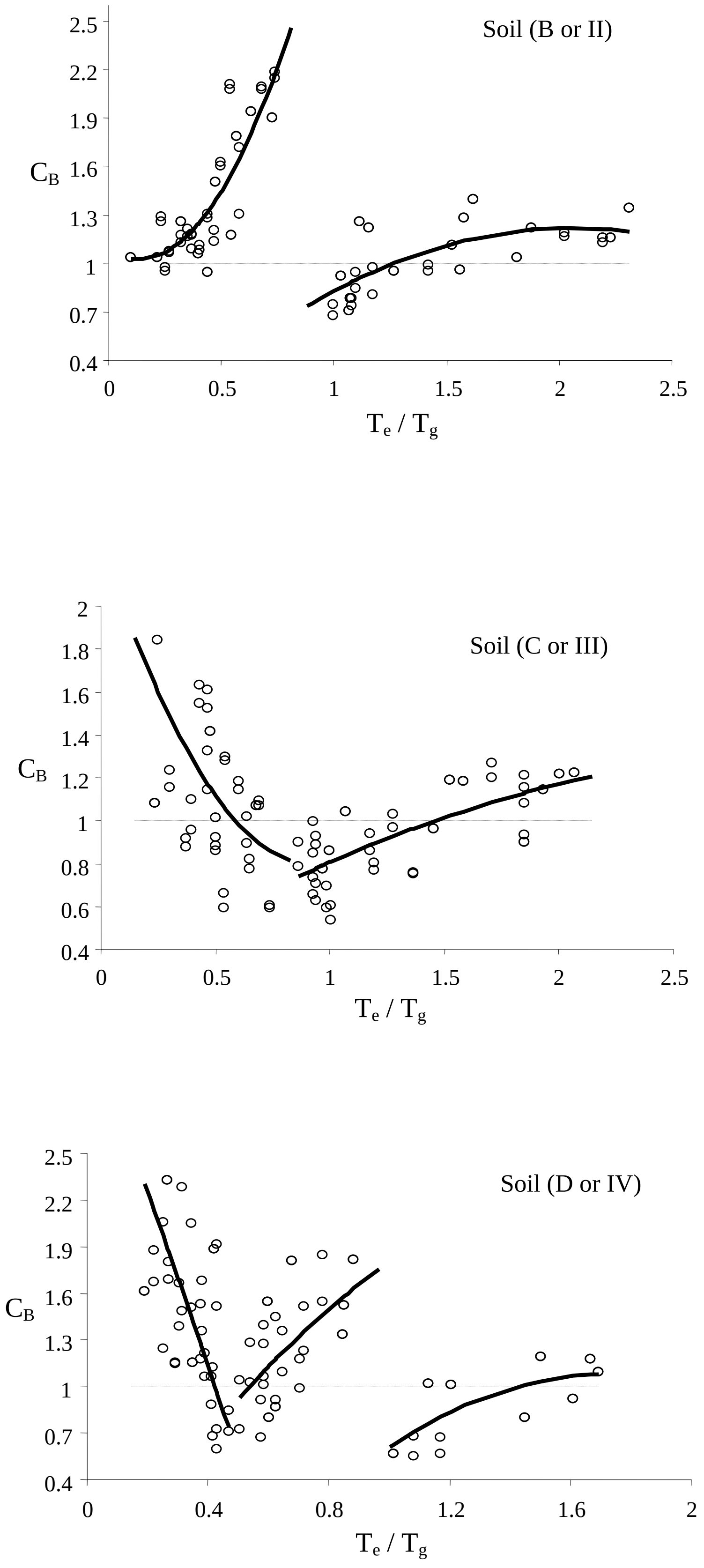

Fig. 17. The coefficient (C_B) curve for soils types.

The validity of the proposed correction factor to estimate target displacement of eight regular concrete bridges with the geometrical specifications depicted in Table 9 was evaluated against the results of NDP. In this table, in the abbreviation B-n-l-h, n: is number of spans, l: span length and h: is pier height.

As before, the earthquake records from the four soil types were selected as input excitations. The target displacement results of employing correction factor to ASCE/SEI 41-06 and original values versus NDP are presented in diagrams of Figure 18 for different soil types. If the two values $(Dis_i)_{NDP}$ and $(Dis_i)_{NSP}$ are equal, the ratio $\frac{(Dis_i)_{NDP}}{(Dis_i)_{NSP}}$ finds the unit, and any other values beyond unit show the larger difference between two estimations. If $\frac{(Dis_i)_{NDP}}{(Dis_i)_{NSP}}$ ratio is denoted as X_i, then $(X_i - 1) \times 100$ may demonstrate the per cent deviation of this ratio in respect to the bisector (shown in lines passing through the origin).

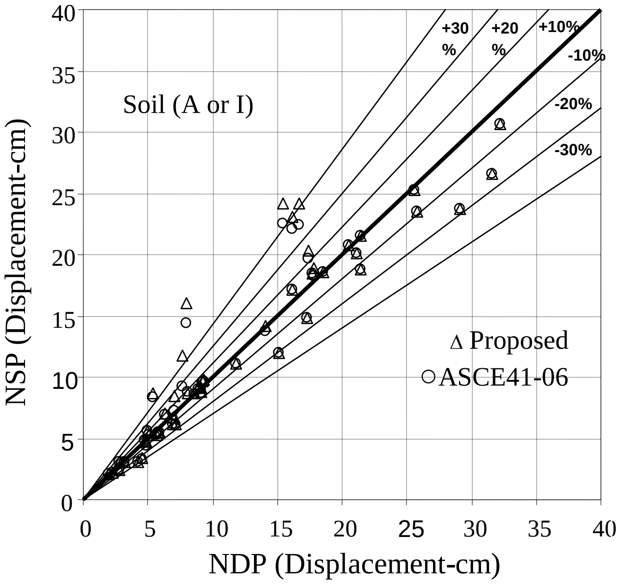

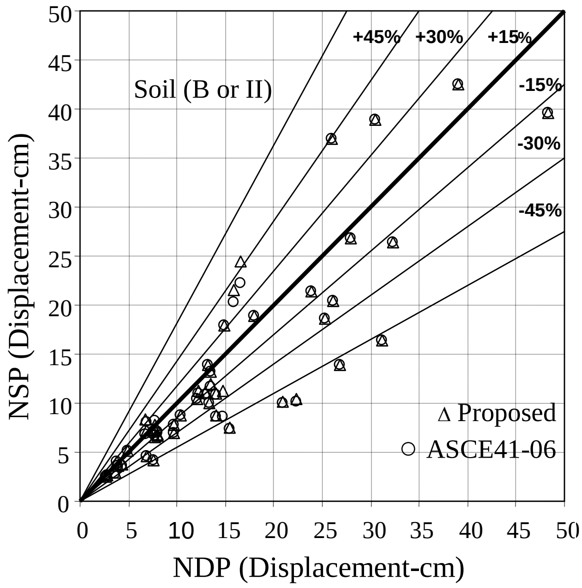

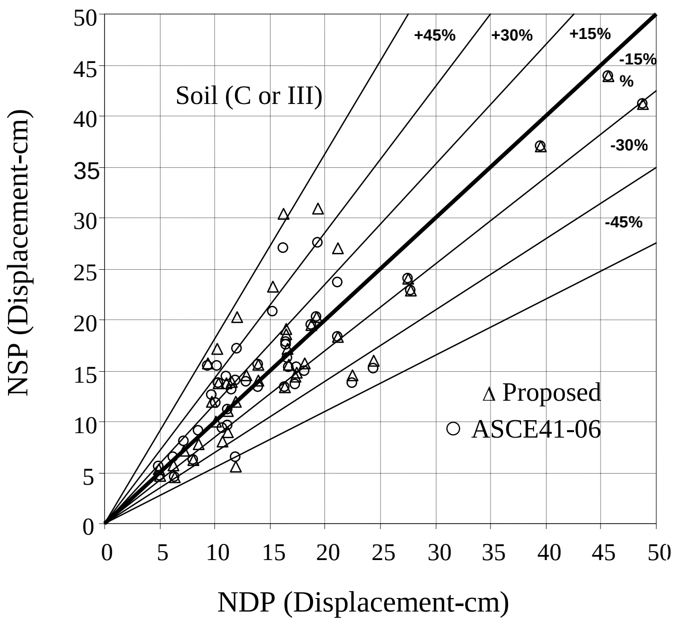

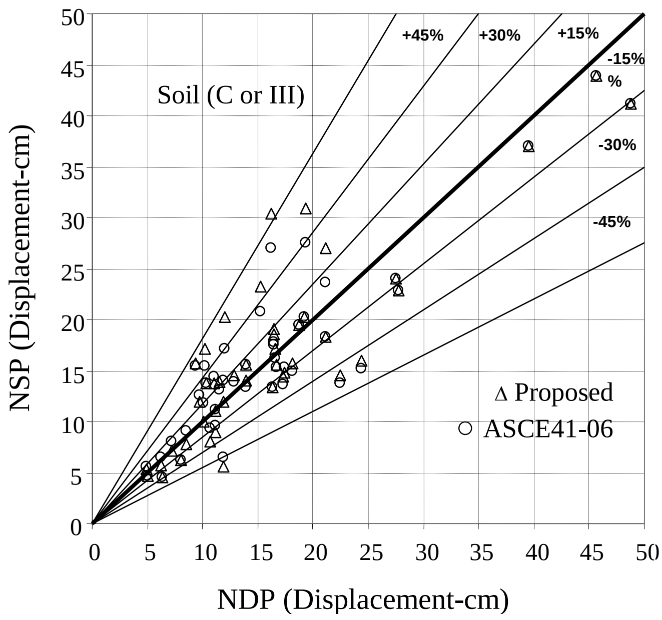

Fig. 18. The accuracy of pushover analysis in estimation of displacement demands for soil types.

Table 9. The bridges selected for evaluation of proposed corrective coefficient validity (C_B) (Jahanfekr, 2011).

B-5-15-5	**B-4-15-5**	**B-3-15-5**	**B-2-15-5**
B-5-15-20	B-4-15-20	B-3-15-12	B-2-15-12

The comparative results show increased accuracy with inclusion of correction factor in Eq. (2) of ASCE/SEI 41-06 for regular concrete bridges for all four types of soil.

CONCLUSIONS

Although ASCE/SEI 41-06 improves the Nonlinear Static Procedures (NSPs) contained in the FEMA 356 for Seismic Rehabilitation of Buildings, examining non-building structures such as bridges indicates this standard cannot successfully improve the target displacement in comparison with NDP. To fulfil this requirement, the correction factor was introduced. This extra coefficient should be multiplied in Eq. (2) of ASCE/SEI 41-06 for regular RC bridges. This coefficient depends simply on the ratio of fundamental effective period to soil predominant period. Due to the closeness of ductility demands for all bridges in this study, the proposed coefficient is free of the nonlinearity mechanism induced by seismic excitation. Further research is needed to evaluate results for irregular bridges and also for other types.

REFERENCES

AASHTO, (2010). *Standard specifications for highway bridges*, American of state Highway and Transportation Officials Inc., Washington, DC.

ASCE/SEI 41-06, (2007). *Seismic rehabilitation of existing building*, American Society of Civil Engineers.

Abdollahzadeh, G. and Malekzadeh, H. (2013). “Response modification factor of coupled steel shear walls”, *Civil Engineering Infrastructures Journal*, 46(1), 15–26.

Aviram, A., Mackie, K., and Stojadinović, B. (2008). *Guidelines for nonlinear analysis of bridge structures in California*, Pacific Earthquake Engineering Research Center, Report No. 2008/03.

Chung, C. Fu. and Alayed, H. (2003). “Seismic analysis of bridges using displacement-based approach”, University of Maryland, TRB Annual Meeting.

Elgamal, A, Yan, Z. and Conte, J.P. (2008). “Three-dimensional seismic response of Humboldt bay bridge-foundation-ground system”, *Journal of Structural Engineering*, ASCE, 134(7), 1165-1176.

Fajfar, P., and Fischinger, M. (1988) “N2 - A method for non-linear seismic analysis of regular buildings”, *Proceedings of the 9th WCEE*, August 2-9, Tokyo-Kyoto, Japan.

FEMA 356, (2000). *NEHRP guidelines for the seismic rehabilitation of buildings*, Federal Emergency Management Agency, Washington, D.C., USA.

FEMA 440, (2005). *Improvement of nonlinear static seismic analysis procedures*, Federal Emergency Management Agency and Applied Technology Council, Washington, D.C., USA.

Fenves, G. L. and Ellery, M. (1998). *Behavior and failure analysis of a multiple-frame highway bridges in the 1994 Northridge earthquake*, Technical Report, Pacific Earthquake Engineering Research Center, University of California, Berkeley, CA.

Freeman, S.A., Nicoletti, J.P. and Tyrell, J.V. (1975) “Evaluations of existing buildings for seismic risk– A case study of puget sound naval shipyard, Bremerton, Washington", *Proceedings of the First U.S. National Conference on Earthquake Engineering*, Oakland, California, 113-122.

Iranian Code of Practice for Seismic Resistant Design of Buildings (Standard No. 2800), 3rd Edition, BHRC Publication No. S–465.

Isakovic, T. and Fischinger, M. (2006). “Higher modes in simplified inelastic seismic analysis of single-column bent viaducts”, *Earthquake Engineering and Structural Dynamics*, 35(1), 95-114.

Jahanfekr, E. (2011). *Comparison of loading pattern on results of nonlinear static (Pushover) analysis of bridges and suggesting for optimum loading*, M.Sc. Dissertation, Faculty of Technical and Engineering, Science and Culture University, Tehran, Iran.

Lestuzzi, P., Schwab, P., Koller, M. and Lacave, C. (2004). “How to choose earthquake recordings for nonlinear seismic analysis of structures”, *13th World Conference on Earthquake Engineering*, Vancouver, B.C., Canada August 1-6, Paper No. 1241.

Lupoi, A., Franchin, P. and Pinto, P.E. (2011). "Further probing of the suitability of pushover analysis for the seismic assessment of bridge structures", University of Rome "Sapienza", Department of Structural and Geotechnical Engineering.

Mander, J.B., Priestley, M.J.N. and Park, R. (1988). “Theoretical stress-strain model for confined concrete", *Journal of the Structural Engineering*, 114(ST8): 1804-1826.

Mazzoni, S., McKenna, F., Scott, M. H., Fenves, G. L. and Jeremic, B. (2013). *Open system for earthquake engineering simulation (OpenSees), Command language manual*, University of California, Berkeley, USA.

Miranda, E. (1993). “Evaluation of site-dependent inelastic seismic design spectra”, *Journal of Structural Engineering*, ASCE, 119(5), 1319-1338.

Paraskeva, S., Kappos, A.J. and sextos, A.G. (2006). “Extension of modal pushover analysis to seismic assessment of bridges", *Earthquake*

Engineering and Structural Dynamics, 35(10), 1269–1293.

PEER Strong Motion Database. (2012). http://peer.berkeley.edu/smcat.

Pinho, R. (2007). “Using pushover analysis for assessment of buildings and bridge”, Course Material for Advanced Earthquake Engineering Analysis- CISM, Udine Italy, 91-120.

Shayanfar, M.A. and Rezaei Abyaneh, R. (2011). “Investigation of lateral load pattern effects on nonlinear static analysis of moment resistant frames”, *Civil Engineering Infrastructures Journal*, 44(5), 607-763.

Shinozuka, M., Feng, M.Q., Kim, H., and Kim, S. (2000). “Nonlinear static procedure for fragility curve development”, *Journal of Structural Engineering*, ASCE, 126(12), 1287-1295.

Yan, Z. (2006). *Sensor data analysis and information extraction for structural health monitoring*, Ph.D. Dissertation, University of California, San Diego.

Zheng, Y., Usami, T. and Hanbin, T. (2003). “Seismic response predictions of multi-span steel bridges through pushover analysis”, *Earthquake Engineering and Structural Dynamics*, 32(8), 1259-1274.